Inelastic neutron scattering study of the hydrogenated (Zr_{55}Cu_{30}Ni_{5}Al_{10})_{99}Y_{1} bulk metallic glass

Andrew Chih-Pin Chuang, Yun Liu, Terrence J. Udovic, Peter K. Liaw, Ge-Ping Yu, and Jia-Hong Huang

Phys. Rev. B **83**, 174206 — Published 25 May 2011

DOI: 10.1103/PhysRevB.83.174206

Inelastic neutron scattering study of hydrogenated $(Zr_{55}Cu_{30}Ni_5Al_{10})_{99}Y_1$ bulk metallic glass

Andrew (Chih-Pin) Chuang[1,2], Yun Liu[3,4], Terrence J. Udovic[3], Peter K. Liaw[2], Ge-Ping Yu[1] and Jia-Hong Huang[1]

[1] Department of Engineering and System Science, National Tsing-Hua University, Hsin-Chu, Taiwan 300
[2] Department of Materials Science and Engineering, University of Tennessee, Knoxville, TN 37996
[3] NIST Center for Neutron Research, National Institute of Standards and Technology, 100 Bureau Drive, MS6102, Gaithersburg, MD 20899-6102, USA
[4] Department of Chemical Engineering, University of Delaware, Newark, DE, 19716, USA

Abstract

The lattice dynamics of both as-charged and room-temperature-aged, hydrogenated bulk metallic glasses (BMG's) with the stoichiometry of $(Zr_{55}Cu_{30}Ni_5Al_{10})_{99}Y_1$ have been investigated by inelastic neutron scattering at 4 K. The vibrational density of states (DOS) of dissolved hydrogen atoms in the as-charged BMG shows a broad band maximized at ~135 meV. Three months of room-temperature aging caused this band to narrow somewhat, losing intensity at both lower and higher energies. The results suggest that hydrogen atoms preferably occupy the interstitial tetrahedral-like t-sites comprised of four Zr atoms, with a local atomic arrangement similar to δ-zirconium hydride. At higher hydrogen loadings, hydrogen atoms can also occupy octahedral-like and/or more Zr-deficient tetrahedral-like o-sites. The spectral differences between the as-charged and aged specimens and accompanying Vicker's hardness measurements suggested that around two-thirds of the hydrogen atoms in the as-charged specimen were trapped in the strongly binding t-sites and relatively immobile at room temperature, while the remaining one-third occupied the more weakly binding o-sites and disappeared from the specimen upon aging. These latter sites most likely play a crucial role in the diffusion of hydrogen in BMG's at room temperature.

Keywords: Inelastic neutron scattering, Amorphous hydride, Bulk Metallic Glasses

Introduction

"Hydrogen in metals" has been a popular topic for material scientists and engineers for many decades. One of the main reasons is the infamous ability of hydrogen to degrade the mechanical properties of most metallic materials[1]. Another reason is the potential of using metal hydrides for hydrogen-storage materials[2-3]. For either perspective, it is very important to understand two fundamental properties, diffusivity and solubility of hydrogen in alloys. The diffusivity determines how rapidly hydrogen can travel within the alloy, and the solubility affects how much hydrogen can be absorbed in the alloy. Both properties are strongly affected by the microstructure of the alloys.

Hydrogen-storage properties of early-transition-metal-late-transition-metal (ETM-LTM) amorphous alloys have been studied extensively since the 1970's. Amorphous alloys tend to have loose atomic packing and more interstitial spaces between atoms. One advantage of amorphous alloys over their crystalline counterparts is their relatively broader range of interstitial-site energies. As a result, they can potentially absorb more hydrogen atoms in a given volume and have higher hydrogen permeation rates[4-5] than the same material in the crystalline state. Another advantage is their large elastic limit, ~ 2%, which could alleviate one of the main problems of current hydrogen-storage materials, the degradation of the material due to a large volume change between the hydrogenation and de-hydrogenation process.

It was found that hydrogen atoms tend to bond with early-transition metals, which have high hydrogen affinity. Samwer et al.[6] studied the structures of amorphous Pd-Zr and Rh-Zr alloys by X-ray diffraction, and suggested that hydrogen only occupied two types of tetrahedral interstitial sites under their experimental conditions. They carefully monitored the Zr-Zr inter-atomic distance as a function of hydrogen concentration and concluded that most of the dissolved hydrogen occupied tetrahedral interstitial sites surrounded by four Zr atoms (E_4 site), and a small part of the hydrogen rested in sites composed of three Zr atoms and one Pd (or Rh) atom (E_3L_1 site, where E denotes early-transition metals, and L denotes late-transition metals). Similar results on the study of ZrNi glasses using neutron diffraction had been reported by Suzuki et al.[7]. They used neutrons to directly probe the hydrogen-metal distance as a function of hydrogen

concentration and indicated the hydrogen atom tended to be four-fold coordinated to either four Zr atoms or three Zr atoms and one Ni atom.[7] Rush et al.[8] came to similar conclusions for the amorphous Ti-Cu system using inelastic neutron scattering (INS). Later, Harris et al.[9] proposed a universal model, after reviewing the common features of hydrogen in Ni-Zr, Cu-Ti, Pd-Zr, Rh-Zr, Cu-Zr, and Fe-Ti systems, to describe the behavior of dissolved hydrogen in ETM-LTM amorphous alloys. They suggested the following; First, interstitial sites for hydrogen are tetrahedral, with varying chemical environments (E_4, E_3L_1, E_2L_2, etc.). Each type of site has different site energy, depending on the affinity of surrounding atoms to hydrogen, and the site energies are broadened due to the distorted atomic environment. Second, the chemical potential of each type of site is independent of composition, and hydrogen can occupy E_4 sites as well as E_3L_1 and E_2L_2 sites. Third, blocking effects exist in the amorphous ETM-LTM-H system, which restrict the maximum fraction of each type of hydrogen absorption site to ~3/8. This site-independent value further predicts the maximum hydrogen/metal (H/M) ratio of 1.9 for this kind of alloy (ETM-LTM).

Studies of hydrogen in bulk metallic glasses (BMGs) have not been done as thoroughly as those for crystalline alloys and binary amorphous ribbons. It was not until the early 1990's that the Zr-based BMG family was discovered[10-11]. This major breakthrough significantly boosted the amount of research on amorphous alloys with an emphasis on being able to synthesize them in large size, which is the first step required for real-world applications. Bulk amorphous metallic alloys exhibit many unique material properties[12-13], leading them to promising materials for various advanced engineering applications[13]. Recently, some of the BMG compositions have drawn considerable attention for their potential as hydrogen purification/separation membranes[4]. Some amorphous alloys that are composed of ETM and LTM were found to have performances comparable to palladium-based membranes and could be cheaper alternatives for hydrogen-selective membranes[4, 14].

In the present study, the vibrational density of states (DOS) of the dissolved hydrogen in $(Zr_{55}Cu_{40}Ni_5Al_{10})_{99}Y_1$(in atomic percent) BMG was investigated by INS. The evolution of neutron vibrational spectra (NVS) as a function of time was studied.

Based on the experimental evidence, a mechanism was proposed to explain the diffusion of hydrogen in ETM-LTM-Al BMG's.

Hydrogen vibrations and inelastic neutron scattering

Hydrogen, composed of one electron and one proton, has the smallest atomic size of all elements in the periodic table. Therefore, it has the potential for a very high mobility in solid metals, even at room temperature. Yet, the small mass and low charge density make it very difficult to be detected by most materials characterization techniques. Fortunately, the relatively large neutron scattering cross section for hydrogen renders the neutron a uniquely useful probe for hydrogen-related studies.

Hydrogen dynamics in a solid can be studied by measuring the energy distribution of scattered thermal neutrons that have exchanged energy with lattice vibrations, thus generating a vibrational DOS. Each absorbed hydrogen atom has its characteristic vibration energies, which correspond to the specific local environment of the interstitial site, such as the nature of coordinating metal atoms, the H-M distances, and the coordination geometry. Hence, the measured DOS can be used as a spectral probe of the distribution of interstitial sites[15]. The above concept had been used extensively to study rare-earth metal hydrides[16-19] and amorphous hydrides[8].

Kirchheim[20] proposed a concept to treat the behavior of hydrogen in amorphous alloys using a term, the density of site energies (DOSE). One can consider an alloy having various types of interstitial sites with different chemical potentials (treated as site energies), and the energy distribution of occupied sites, $n_i(E)$, in an amorphous alloy follows a Gaussian function

$$n_i(E) = \frac{1}{\sigma\sqrt{\pi}} \exp\left[-\left(\frac{E - E_i}{\sigma^2} \right)^2 \right] \tag{1.1}$$

where σ is the full width at half maximum (FWHM) of the distribution, E_i is the site energy for the i^{th} kind of site, and $n(E)$ fulfill the following normalization condition.

$$\int_{-\infty}^{\infty} n(E)dE = 1 \tag{1.2}$$

The distribution of hydrogen occupying a specific site with a site energy E_i follows Fermi Dirac statistics.

$$f(E) = \frac{1}{1+e^{((E-E_i)/k_BT)}} \tag{1.3}$$

where k_B is Boltzmann's constant, and T is the temperature in Kelvin. By further integrating DOSE over all energies, one can obtain the total fraction, N/N_o, of sites occupied by hydrogen

$$\frac{N}{N_0} = \int_{-\infty}^{\infty} f(E)n(E)dE = \int_{-\infty}^{\infty} \frac{n(E)}{1+e^{((E-E_i)/k_BT)}}dE \tag{1.4}$$

where N is the total number of dissolved hydrogen atoms, and N_0 is the total number of available sites. For BMG's, the precise prediction of this ratio is not straightforward, since a good value for N_0 requires an accurate structure model for BMG's. Nevertheless, the DOSE picture is quite useful to analyze hydrogen in amorphous alloys[21].

Experimental details

The $(Zr_{55}Cu_{40}Ni_5Al_{10})_{99}Y_1$ bulk amorphous alloys were fabricated in an atmosphere-controlled arc melter by a suction-casting method[22]. The master ingot of the alloy was prepared by arc-melting the mixture of high-purity transition metals, Zr (> 99.95 % mass fraction), Cu (99.99 %), Ni (99.995 %), Al (99.9995 %), and Y (99.5 %) in a water-cooled copper crucible under an argon atmosphere. Then, the ingot was re-melted several times before being ejected into a water-cooled copper mold to produce 12 x 2 x 30 mm plates. A more detailed fabrication procedure can be found elsewhere[22]. All fast-cooled specimens used in the experiments were examined by high-energy X-ray diffraction (XRD) in transmission geometry and differential-scanning calorimetry (DSC).

All specimens showed a lack of sharp diffraction peaks by XRD and a distinct, reproducible glass transition point by DSC.

The hydrogen charging of the specimens was conducted by a cathodic-charging method at room temperature. There are several ways to introduce hydrogen into materials, many of which involve either high temperatures or high pressures. Since amorphous alloys are in a meta-stable state, which may crystallize at high temperature, cathodic-charging in an aqueous solution in atmosphere is one of the most common ways to introduce hydrogen into amorphous alloys. The specimens were charged continuously for 36 hours with a constant current density of 30 mA/cm^2 in the 0.5N H_2SO_4 solution at room temperature with 0.1 % mass fraction As_2O_3 as the hydrogen-uptake promoter. Prior to the charging process, all specimens were wet-grounded with SiC papers down to 800 grit, then polished with Al_2O_3 powders down to 1 μm, and finally rinsed with acetone. Although the alloy is susceptible to hydrogen damage in a long duration of a high-charging-current density, the specimens were still macroscopically coherent solids within the charging time and current density used in this study. After the hydrogenation process, part of the specimens, which were used in the neutron experiment, were transferred to a He-filled box, and sealed in an Al cylinder, and immediately dipped into liquid nitrogen to alleviate any possible hydrogen escape. Part of the specimens was used to collect the hardness data. The hardness of the sample was measured by a Vickers micro-hardness tester with an indentation load of 100 gf. The measurement was conducted right after the charging process (within 12 h) and repeated after 17 h, 38 h, and 3 mos. aging treatment in atmospheric air.

The INS measurements were conducted at the National Institute of Standards and Technology Center for Neutron Research (NCNR). Neutron vibrational spectra (NVS) were obtained using the BT-4, Filter Analyzer Neutron Spectrometer (FANS)[23] with the Bi-Be-graphite-Be composite filter analyzer and an averaged neutron final energy of 1.2 meV. The horizontal collimations before and after the Cu(220) monochrometer were both 40‘ of arc. The measured spectra ranged from 40 meV to 200 meV with an energy resolution of 4 % to 5 % of the incident energy. The spectra were taken at 4 K for the as-cast and as-charged specimens. After NVS measurements, the aged specimen was stored

in a dry box, in atmospheric air. After three months, the same measurement was repeated again for this specimen.

Results and Discussion

The NVS of the as-cast (without hydrogenation), the as-charged (hydrogenated), and the three-months-aged (hydrogenated) $(Zr_{55}Cu_{40}Ni_5Al_{10})_{99}Y_1$ BMG at 4 K are shown in Figure 1. The spectra of the as-cast specimen with no hydrogen content showed a featureless background within the observed energy range (i.e., the intensity of the vibrational DOS of the amorphous alloy alone is very small due to the relatively small neutron scattering cross sections of the other elements in the as-cast sample.), confirming that under the current experimental conditions, all the spectral features for the hydrogenated specimens were due to the vibrational DOS of absorbed hydrogen. Similar to the previously reported amorphous hydride systems[8], the NVS of both as-charged and aged samples exhibited a broad (~50 meV FWHM) energy distribution maximized at ~135 meV. The spectra in Figure 1 are scaled to the same neutron monitor counts, providing a direct comparison of H concentrations. In particular, the relative integrated intensities reflect the relative total H concentrations in the as-charged and aged states, clearly indicating a decrease in H concentration upon aging. The bottom panel of Figure 1is the difference spectrum between the as-charged and aged samples. This spectrum shows two maxima near ~100 meV and ~170 meV, indicating that the spectrum of the as-charged sample is actually comprised of three broad bands, a main band in the middle with two minor side bands at higher and lower energies. The difference spectrum clearly indicates that the aged sample has lost these minor side bands, leaving the main middle band essentially intact.

Since the DOSE in amorphous alloys can be expressed by a Gaussian function (Eq. 1.1), we obtained good Gaussian fits for each of the three bands for the as-charged sample and the remaining band for the aged sample. The fitted curves are shown in Figure 2, and the fit parameters are listed in Table I. Our results are further compared with the NVS of crystalline zirconium hydrides reported by others, as summarized in Table II. For the as-charged sample, the fit resulted in a main peak centered at 135 meV

and two minor side peaks centered at 97 meV and 168 meV. For the aged sample, the fit resulted in a single main peak with a similar position (134 meV) and integrated intensity as that for the as-charged sample, indicating (and consistent with the Figure 1 difference spectrum) that the amount of interstitial hydrogen associated with this feature indeed did not change with room-temperature aging. Thus, this hydrogen appears to be relatively strongly bound, immobile, and effectively trapped at room temperature.

Previous theoretical simulations using the central force lattice dynamic model (CF model) suggested that the hydrogen-vibration energy of a particular occupation site only depends on the H-M distance as well as the local atomic arrangement (the site geometry) [24]. The peak width is mainly determined by the interaction of the surrounded M atoms to the second-nearest M atoms. Therefore, the width of the DOSE in amorphous alloys is wider than that in crystalline alloys with the same chemical composition[8]. As a result, the site energy is independent of hydrogen concentration. According to previous results[8,24-29] and after comparing the DOSE of hydrogen in BMG's with several other well-known crystalline zirconium hydrides in Table II, we believe that the main 135 meV band reflects hydrogen mainly in tetrahedral interstices (t-sites) composed of four Zr atoms, and the short-range-order (SRO) bonding of the BMG is almost identical to the bonding arrangements in f.c.c zirconium hydride. Our results bolster the argument that the Zr_4 tetrahedron is one of the basic structures composing Zr-based BMG's. Although it is likely that the Zr_4 tetrahedron is the strongest binding tetrahedral interstice in this BMG, this does not rule out the possibility that other potential Zr-rich tetrahedral interstices, such as Zr_3Ni, contribute to the collection of room-temperature hydrogen-trapping sites available and yield similar H vibrational energies as the Zr_4 t-sites. Further research is required to determine in more detail the populations and relative binding energies of the other types of possible t-sites.

Besides the strongly binding t-sites, it is clear from the presence and behavior of the minor side bands at 97 meV and 168 meV for the as-charged sample that additional more weakly binding hydrogen sites are occupied. Their relative intensities compared to the main t-site feature indicate that around one-third of the interstitial hydrogen atoms are in these types of sites. The lower-energy side band is in the expected spectral region for

hydrogen atoms occupying octahedral-like sites[24] (also tentatively labelled o-sites with reasons given later), since octahedral sites are typically larger interstices than tetrahedral sites. It is not certain what other type of interstitial sites (also tentatively labelled o-sites to distinguish them from the more strongly binding t-sites) might be responsible for the higher-energy side band. Based on the approximate 2:1 intensity ratio of the lower-energy and higher-energy side bands, it is tempting to associate both bands to the same types of octahedral-like sites. Hydrogen in these sites could have two degenerate basal-plane vibrations at lower energy and one non-degenerate orthogonal apical vibration at higher energies. This is commonly observed for octahedral sites comprised of more than one type of metal atom and/or possessing geometric site distortion, such as for Nb_4V_2 and V_6-octahedral sites in $Nb_{95}V_5H_x$ and β-V_2H, respectively[39,40] Of course, since this is an amorphous alloy, we cannot rule out that the two side bands are not at least partially associated with hydrogen in two different sites such other octahedral-like sites (e.g., Zr_4Ni_2)[41] and/or more Zr-deficient tetrahedral-like sites (e.g., Zr_2Ni_2, Zr_2Cu_2, etc.). Again, the exact local geometry of the o-sites in the BMG requires further research.

Compared to the trapped t-site hydrogen, the spectroscopic results indicate that the o-site hydrogen atoms are clearly more mobile and can move more freely at room temperature. Moreover, the hydrogen jumping rate between o-sites is probably orders of magnitude higher than the jumping rate between t-sites or from t-sites to o-sites. This finding suggests that the o-site hydrogen could play an important role in the elementary diffusion process of hydrogen in BMG's at room temperature.

Finally, Figure 3 presents the Vicker's hardness of the hydrogenated $(Zr_{55}Cu_{40}Ni_5Al_{10})_{99}Y_1$ as a function of aging time (293 K, room-temperature aging). The time denotes the duration after electrochemical charging. The hardness of the sample shows an abrupt 32% increase from 490 HV to 650 HV right after hydrogen charging, and decreases parabolically until it becomes stable at ~560 HV after ~20 d. The hydrogen-induced hardening of BMG's has been reported on Zr-based systems[30], La-based systems[31], and Mg-based systems[32]. For such systems without crystalline-hydride formation after hydrogenation, the increased hardness was proposed to be a consequence of the hydrogen-absorption-induced decrease in free volume in the material, which was

causing the retardation of atomistic relaxation processes[30]. The magnitude of the increase was found to be proportional to the hydrogen concentration in the sample[30]. The current result suggests that one might indeed use the hardness as an index to qualitatively estimate the hydrogen concentration in the sample and is consistent with the spectroscopic observations. In other words, the decrease in hardness with time followed by its stabilization mirrors the loss of the initially dissolved hydrogen that was associated with the more weakly binding o-sites, eventually leaving behind the rest of the hydrogen trapped in the t-sites.

Conclusion

The lattice dynamics of both as-charged and room-temperature-aged hydrogenated $(Zr_{55}Cu_{30}Ni_5Al_{10})_{99}Y_1$ BMG's have been investigated by inelastic neutron scattering. Comparison of the optical vibrational densities of states of dissolved hydrogen atoms in the as-charged and aged alloy suggests that the hydrogen atoms preferentially occupy strongly binding, tetrahedral-like interstices (t-sites) comprised totally or mostly of Zr atoms and subsequently fill more weakly binding, Zr-deficient and/or octahedral-like interstices (o-sites) as the hydrogen concentration in the alloy exceeds a certain level. The spectral data combined with hardness measurements suggest that the Zr-rich t-sites act as hydrogen traps, forming a stable amorphous hydride phase at room temperature. The hydrogen-occupied Zr_4 t-sites in the BMG are most likely very similar to the local atomic arrangement of δ-zirconium hydride (f.c.c), suggesting that the short-range order in the BMG is very similar to the order in its crystalline counterpart. The changes of the neutron vibrational spectra between as-charged and aged specimens imply that hydrogen atoms in the t-sites are much less mobile than those occupying the o-sites. These results suggest that these more weakly binding o-sites in the BMG play a crucial role in the diffusion of hydrogen at room temperature.

Acknowledgement:

The authors would like to acknowledge the financial support from the National Tsing-Hua University at Hsin-Chu, Taiwan, and the National Science Foundation (NSF), the International Materials Institutes (IMI) Program (DMR-0231320, DMR-0421219, DMR-0909037, and CMMI-0900271). Dr. J.J. Rush of the National Institute of Standards and Technology (NIST) is also appreciated for his useful advice and discussion.

Reference:

[1] H. K. Birnbaum, in *Hydrogen effects on material behavior, TMS*, edited by N. R. Moody and A. W. Thompson (TMS, Warrendale, 1990), p. 639.

[2] G. W. Crabtree, M. S. Dresselhaus, and M. V. Buchanan, Physics Today **57**, 39 (2004).

[3] B. Sakintuna, F. Lamari-Darkrim, and M. Hirscher, International Journal of Hydrogen Energy **32**, 1121 (2007).

[4] M. D. Dolan, N. C. Dave, A. Y. Ilyushechkin, L. D. Morpeth, and K. G. McLennan, Journal of Membrane Science **285**, 30 (2006).

[5] S. I. Yamaura, S. Nakata, H. Kimura, and A. Inoue, Journal of Membrane Science **291**, 126 (2007).

[6] K. Samwer and W. L. Johnson, Phys. Rev. B **28**, 2907 (1983).

[7] K. Suzuki, N. Hayashi, Y. Tomizuka, T. Fukunaga, K. Kai, and N. Watanabe, Journal of Non-Crystalline Solids **61-2**, 637 (1984).

[8] J. J. Rush, J. M. Rowe, and A. J. Maeland, Journal of Physics F-Metal Physics **10**, L283 (1980).

[9] J. H. Harris, W. A. Curtin, and M. A. Tenhover, Phys. Rev. B **36**, 5784 (1987).

[10] A. Peker and W. L. Johnson, Applied Physics Letters **63**, 2342 (1993).

[11] A. Inoue, T. Zhang, N. Nishiyama, K. Ohba, and T. Masumoto, Materials Transactions Jim **34**, 1234 (1993).

[12] W. L. Johnson, Mrs Bulletin **24**, 42 (1999).

[13] A. Inoue, Acta Mater. **48**, 279 (2000).

[14] D. Dudek, (Elsevier Science Sa, 2007), p. 152.

[15] R. Hempelmann and J. J. Rush, (Plenum Publishing Corp., New York, 1986).

[16] I. S. Anderson, J. J. Rush, T. Udovic, and J. M. Rowe, Physical Review Letters **57**, 2822 (1986).

[17] T. J. Udovic, J. J. Rush, and I. S. Anderson, Journal of Alloys and Compounds **231**, 138 (1995).

[18] T. J. Udovic, J. J. Rush, Q. Huang, and I. S. Anderson, Journal of Alloys and Compounds **253**, 241 (1997).

[19] T. J. Udovic, Q. Huang, and J. J. Rush, Phys. Rev. B **61**, 6611 (2000).

[20] R. Kirchheim, Acta Metallurgica **30**, 1069 (1982).

[21] R. Kirchheim, Progress in Materials Science **32**, 261 (1988).

[22] J. J. Wall, C. Fan, P. K. Liaw, C. T. Liu, and H. Choo, Rev. Sci. Instrum. **77**, 4 (2006).

[23] T. J. Udovic, et al., Nuclear Instruments & Methods in Physics Research Section a-Accelerators Spectrometers Detectors and Associated Equipment **588**, 406 (2008).

[24] E. L. Slaggie, Journal of Physics and Chemistry of Solids **29**, 923 (1968).

[25] S. S. Pan and F. J. Webb, Nucl. Sci. Eng. **23**, 194 (1965).

[26] J. G. Couch, O. K. Harling, and L. C. Clune, Phys. Rev. B **4**, 2675 (1971).

[27] R. Khodabakhsh and D. K. Ross, Journal of Physics F-Metal Physics **12**, 15 (1982).

[28] I. Pelah, C. M. Eisenhauer, D. J. Hughes, and H. Palevsky, Physical Review **108**, 1091 (1957).

[29] K. Kai, S. Ikeda, T. Fukunaga, N. Watanabe, and K. Suzuki, Physica B & C **120**, 342 (1983).
[30] D. Suh and R. H. Dauskardt, Scripta Materialia **42**, 233 (2000).
[31] C. P. Chuang, J. H. Huang, W. Dmowski, P. K. Liaw, R. Li, T. Zhang, and Y. Ren, Applied Physics Letters **95** (2009).
[32] C. P. Chuang, J. H. Huang, W. Dmowski, and P. K. Liaw, (unpublished results).
[33] A. I. Kolesnikov, I. O. Bashkin, A. V. Belushkin, E. G. Ponyatovsky, and M. Prager, Journal of Physics-Condensed Matter **6**, 8989 (1994).
[34] A. I. Kolesnikov, I. O. Bashkin, A. V. Belushkin, E. G. Ponyatovsky, M. Prager, and J. Tomkinson, Physica B-Condensed Matter **213**, 445 (1995).
[35] S. S. Pan, W. E. Moore, and M. L. Yeater, Transactions of the American Nuclear Society **9**, 495 (1966).
[36] S. Ikeda, N. Watanabe, and K. Kai, Physica B & C **120**, 131 (1983).
[37] S. S. Malik, D. C. Rorer, and G. Brunhart, Journal of Physics F-Metal Physics **14**, 73 (1984).
[38] R. Hempelmann, D. Richter, and B. Stritzker, Journal of Physics F-Metal Physics **12**, 79 (1982).
[39] R. Hempelmann, D. Richter, J. J. Rush, and J. M. Rowe, J. Less-Common Metals, **172-174**, 281 (1991).
[40] T. J. Udovic, J. J. Rush, R. Hempelmann, and D. Richter, J. Alloys Compds. **231**, 144 (1995).
[41] H. Wu, W. Zhou, T. J. Udovic, J. J. Rush, T. Yildirim, Q. Huang, and R. C. Bowman, Jr., Phys. Rev. B **75**, 064105 (2007).

Table I. Peak position, FWHM, amplitudes, and peak areas of the Gaussian functions that were used to fit the DOS of hydrogen in $(Zr_{55}Cu_{40}Ni_5Al_{10})_{99}Y_1$. (N.B.: the spectral energy resolutions at 84 meV, 97 meV, and 135 meV are 3.6 meV, 4.4 meV, and 7.1 meV, respectively.)

Sample Condition	H site	Center E_i (meV)	FWHM 2σ (meV)	Peak Height	Peak Area	Peak Area %	Υ^2-coef.
As-charged	o-site	97	67	0.0023	0.1652	23	0.9964
	t-site	135	44	0.0097	0.4632	64	
	o-site	168	49	0.0020	0.0956	13	
Aged	t-site	134	42	0.0102	0.4732	100	0.9942

Table II Comparison of optical vibrational peaks of hydrogen atoms in various zirconium hydrides and the BMG.

Material	H occupation site	Peak Center E_i (meV)	FWHM □□ (meV)	notes	Ref.
$(Zr_{55}Cu_{40}Ni_5Al_{10})_{99}Y_1$	o-site	97	45.562	(4 K) as-charged present work	*
	t-site	135	51.446		
	o-site	168	34		
	t-site	134	4644.0	(4 K) aged, 3 months	
δ-ZrH	Tetra.	134	15	(298 K) (f.c.c)	[28]
γ-ZrH	Tetra.	142,149,156	<10	(4.5 K) (f.c.o)	[33-34]
ZrH_2	Tetra.	137	20	(298 K)	[35]
ε-ZrH_2	Tetra.	137,143,154	20~25	(298 K) (f.c.t)	[26, 36]
ε-ZrH_x	Tetra.	132,137,151	10~20	(77 K) (f.c.t)	[37]
α-$ZrH_{0.03}$	Tetra.	143	-	(490 K) (h.c.p)	[38]
α-$ZrH_{0.03}$	Tetra.	144	47	(873 K) (h.c.p)	[27]
ZrH_2	Tetra.	137	20	(296 K) calculated by CF model, assuming CaF_2 structure	[24]

* Current study

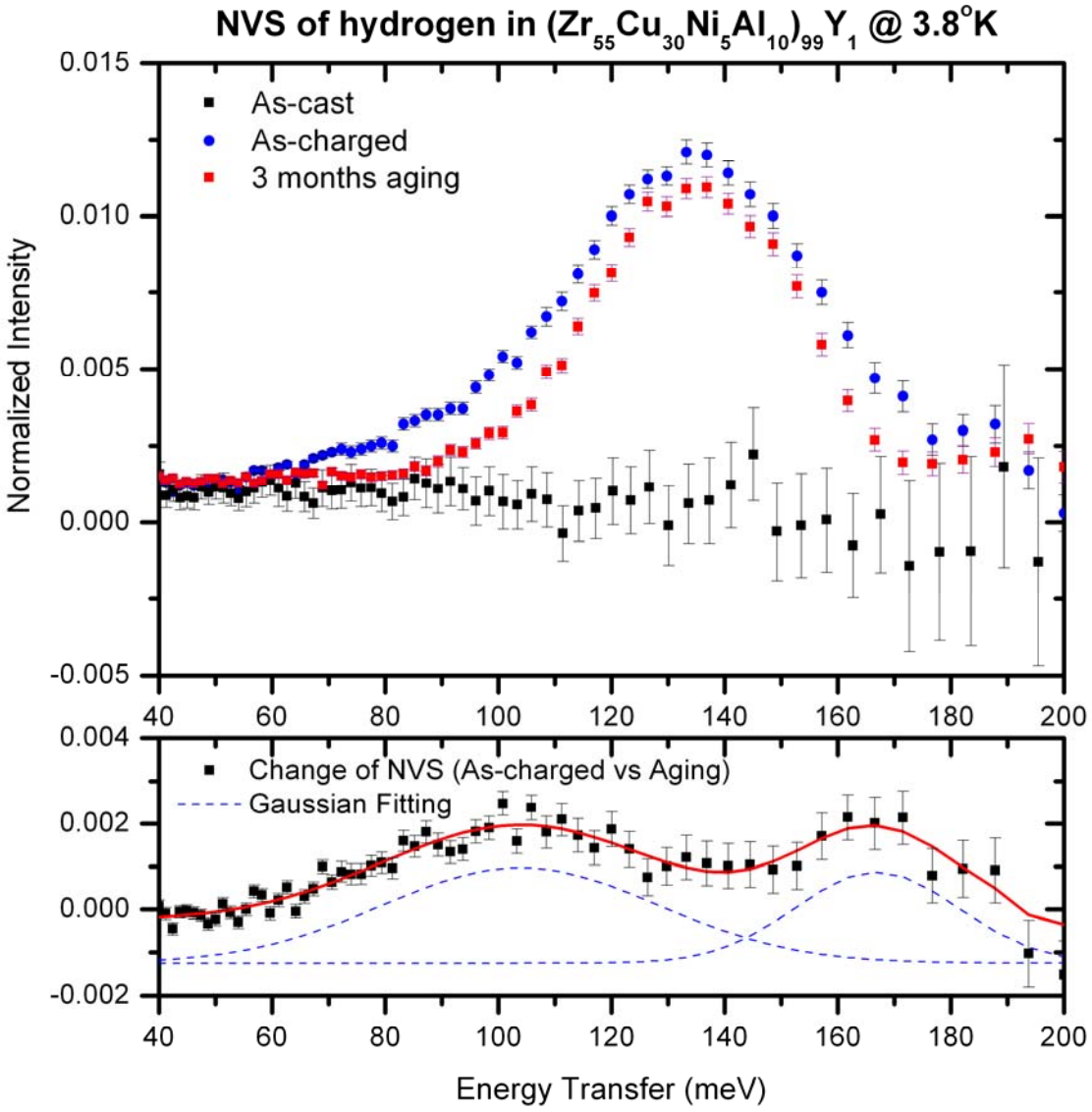

Figure 1. (Color online) (top) NVS at 4 K of an as-cast, hydrogen-charged, and aged hydrogenated $(Zr_{55}Cu_{40}Ni_5Al_{10})_{99}Y_1$ bulk amorphous alloy. (bottom) The loss of hydrogen vibrational DOS due to 3 months aging treatment.

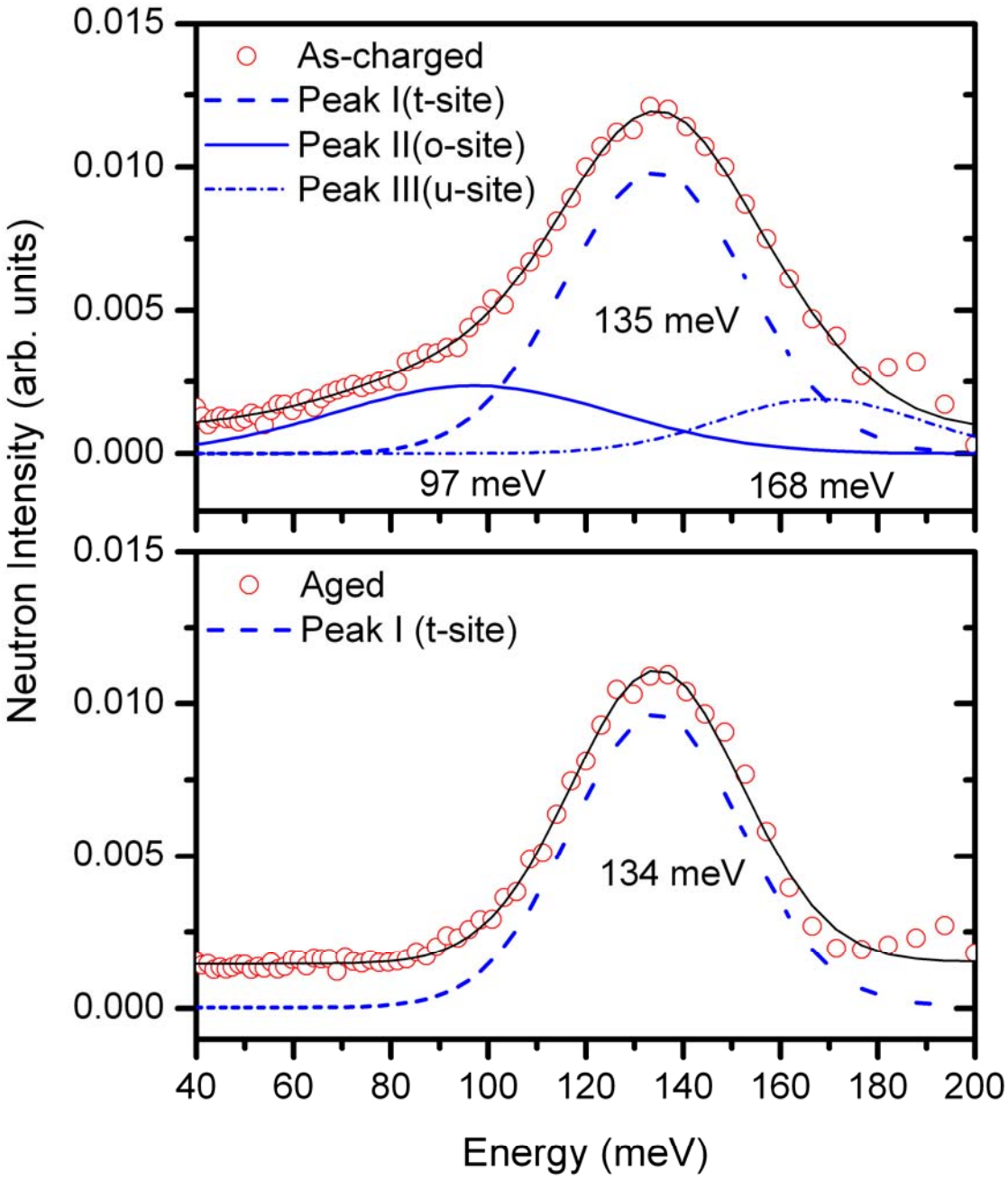

Figure 2 (Color online) Experimental (open points) and calculated (line) spectra of the as-charged and aged samples in the range of the hydrogen optical modes.

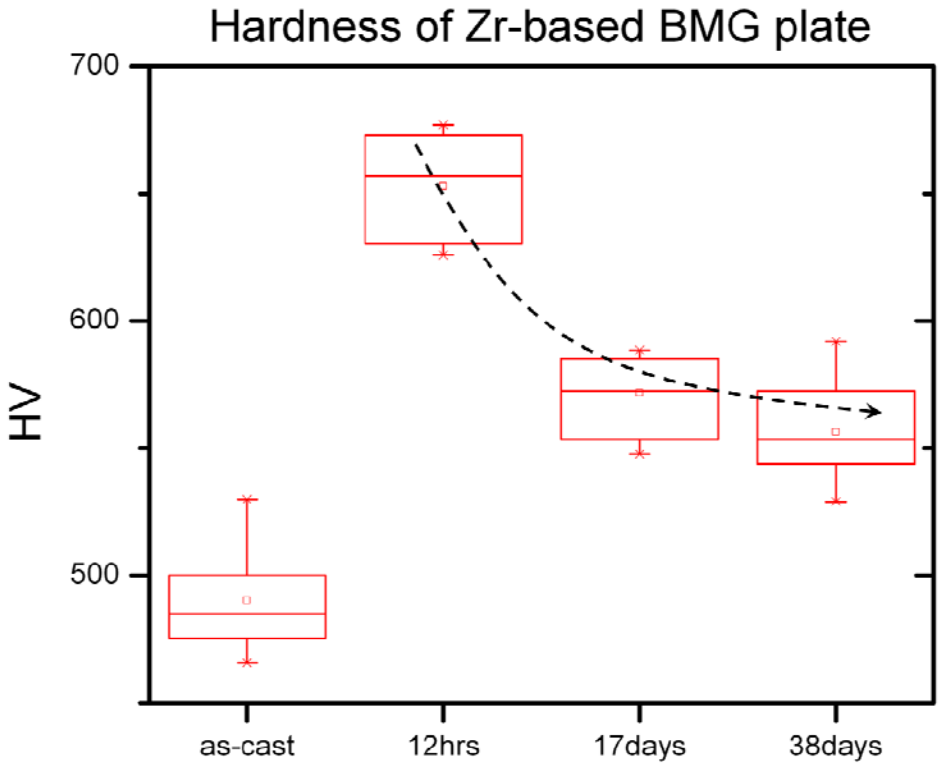

Figure 3 (Color online) Vicker's hardness of hydrogenated $(Zr_{55}Cu_{40}Ni_5Al_{10})_{99}Y_1$ as a function of aging time at 293 K. The time denotes the duration after hydrogen charging.